

A spectral method for dispersive solutions of the nonlocal Sine-Gordon equation

A. Coclite^a, L. Lopez^{b,*}, S. F. Pellegrino^a

^a*Dipartimento di Ingegneria Elettrica e dell'Informazione (DEI), Politecnico di Bari,
Via Re David 200 – 70125 Bari, Italy*

^b*Dipartimento di Matematica, Università degli Studi di Bari,
Via Orabona 4 – 70125 Bari, Italy*

Abstract

Moved by the pressing need for rigorous and reliable numerical tools for the analysis of peridynamic materials, the authors propose a model able to capture the dispersive features of nonlocal soliton-like solutions obtained by a peridynamic formulation of the Sine-Gordon equation. The analysis of the Cauchy problem associated to the peridynamic Sine-Gordon equation with local Neumann boundary condition is performed in this work through a spectral method on Chebyshev polynomials nodes joined with the Störmer-Verlet scheme for the time evolution. The choice for using the spectral method resides in the resulting reachable numerical accuracy, while, indeed, Chebyshev polynomials allow straightforward implementation of local boundary conditions. Several numerical experiments are proposed for thoroughly describe the ability of such scheme. Specifically, dispersive effects as well as the ability of preserving the internal energy of the specific peridynamic kernel are

*Corresponding author

Email addresses: alessandro.coclite@poliba.it (A. Coclite),
luciano.lopez@uniba.it (L. Lopez), sabrinafrancesca.pellegrino@poliba.it (S. F. Pellegrino)

demonstrated.

Keywords: Peridynamics, Nonlocal Sine-Gordon, Spectral Methods, Nonlocal Solitons, Numerical Methods.

2020 MSC: 74A70, 74B10, 70G70, 35Q70

Introduction

The Sine-Gordon Equation is a nonlinear partial differential equation that describes one-dimensional waves in a continuous media. It is often seen in various field theories, such as condensed matter physics and nonlinear optics. In the one-dimensional case, it is an example of a completely integrable system, meaning that the equation possesses an infinite number of conservation laws and that its solutions can be written in terms of spectral parameters through the inverse scattering method [1–5]. This property leads to exact solutions of the Sine-Gordon equation, known as solitons. Solitons are stable and localized nonlinear waves that retain their shape as they propagate. They have a crucial importance both in mathematics and physics since many physical systems present soliton-like behaviors. Solitons are widely seen in the theory but also exist as sound waves in nonlinear materials and as kinks or domain walls in nano-magnetic materials. The Sine-Gordon equation reads:

$$\partial_{tt}^2 u(x, t) - c^2 \partial_{xx}^2 u(x, t) + \sin(u(x, t)) = 0, \quad (0.1)$$

with $x \in \mathbb{R}$ and $t \in \mathbb{R}^+ \setminus \{0\}$ being the spatial and temporal coordinates, respectively. $u(x, t)$ the displacement field and c the propagation speed. The choice of the nonlinear forcing term $\sin(u(x, t))$ allows for the formation of

solitons. Long-range interactions and memory effects can be introduced through an additive integral term to $\sin(u(x, t))$ accounting for the global influence on the solution at a point [6–8]:

$$\partial_{tt}^2 u(x, t) - c^2 \partial_{xx}^2 u(x, t) + \sin(u(x, t)) - \int_{-\infty}^{\infty} S(x-y) \sin(u(y, t)) dy = 0. \quad (0.2)$$

$S(x - y)$ is a nonlocal kernel regulating the influence of the entire spatial domain on the wave dynamics. The specific form of such kernel defines range and character of nonlocal interactions. Eq.(0.2) often exhibits interesting and rich dynamics, and its solutions can involve the formation of various types of localized structures, including the so-called nonlocal solitons [9–11]. Indeed, nonlocality can be prescribed also for the wave internal response function $\partial_{xx} u(x, t)$ by promoting the local Laplace operator to an integral operator. This theory is called peridynamics and corresponds to a nonlocal mechanics continuum theory extending local elasticity to long-range interactions thus accounting for material discontinuities, damages and failures [12–22]. The peridynamic Sine-Gordon equation reads:

$$\partial_{tt}^2 u(x, t) - \mathcal{L}(u(\cdot, t))(x) + \sin(u(x, t)) = 0, \quad (0.3)$$

where $\mathcal{L}(u(\cdot, t))$ is the peridynamic kernel. As well-known, traditional continuum mechanics constitutive equations rely on spatial gradients of displacements and stresses. On the contrary, within peridynamic framework, the material internal energy is defined by integral (and often fractional) operators involving information from a region around a given point usually referred as *peridynamic horizon*. Moreover, the integro-differential nature

of Eq. (0.3) depicts the material dynamics at several scales at the same time. This feature lies in its ability to capture the effects of small-scale features on the overall behavior of the solution [23–25]. The synergy between nonlocal differential equations and multiscale modeling enhances the ability to simulate and understand complex physical phenomena occurring in materials and systems with intricate structures and behaviors across multiple scales. The complexity of the peridynamic operator would often require the use of raffinate numerical tools for approximating the evolution of the system in time. In the last two decades the increasing interest in peridynamics grossly divided the researchers in two main directions: finite element models [26–31] and mesh-free methods [32–35] or quadrature methods [36, 37]. Only in the very last years spectral methods [38–43] and boundary element methods [44] have been developed enlarging the range of suitable numerical tools. Indeed, due to the convergence properties of different numerical scheme, mesh-free and quadrature methods are commonly chosen when dealing with nonlinear kernels; on the contrary, spectral methods and boundary element methods are usually chosen for accurate numerical solutions of complex semilinear or linear peridynamics. As per finite elements discretization, the number of proposed schemes in literature is so large and so diverse that a main application is hard to find. Moreover, the specific formulation of a peridynamic equation, including the choice of the kernel function and the underlying assumptions, may vary based on the requirements of the specific application or material being studied. As the matter of facts, by combining some grandstanding ingredients such as, nonlocality, fractionality, nonlinearity and singularity, the ability of a specific peridynamic kernel is defined [45].

In this paper we consider the linear fractional one-dimensional kernel proposed and discussed in [46]:

$$\mathcal{L}u(x, t) = \int_{B_\delta(x)} f(x-x', u(x, t)-u(x', t)) dx' = \int_{B_\delta(x)} \frac{u(x, t) - u(x', t)}{|x - x'|^{1+2\alpha}} dx', \quad (0.4)$$

with $\alpha \in (0, 1)$ and $B_\delta(x)$ being the interval centered on x by radius δ . This choice is motivated under the following four physically-sound constitutive assumptions for the pairwise force interaction $f : \mathbb{R} \times (\mathbb{R} \setminus \{0\}) \rightarrow \mathbb{R}$:

- $f \in C^1(\mathbb{R} \times (\mathbb{R} \setminus \{0\}); \mathbb{R})$,
- $f(x-x', u(x)-u(x')) = f(x'-x, u(x)-u(x'))$ for every $(x-x', u(\cdot, t)) \in \mathbb{R} \times (\mathbb{R} \setminus \{0\})$,
- $f(x-x', u(x)-u(x')) = -f(x'-x, u(x')-u(x))$ for every $(x-x', u(\cdot, t)) \in \mathbb{R} \times (\mathbb{R} \setminus \{0\})$,
- there exists a function $\Phi \in C^2(\mathbb{R} \times (\mathbb{R} \setminus \{0\}))$ such that $\Phi = \nabla_u f$.

Due to the choice made for the pairwise force interaction, the energy space is H^α and $\mathcal{L}u(x, t)$ corresponds to the fractional-censurated α -Laplacian (α being the fractionality parameter). The analysis of the evolutionary problem associated to Eq.(0.3) with local Neumann boundary condition is addressed here by adopting the spectral method approach on Chebyshev polynomials nodes while the temporal integration is demanded to the Störmer-Verlet scheme, thus returning a suitable, efficient and accurate computational tool [39, 40, 43]. This method is peculiarly suited for integral operator that can be expressed as convolution product so that preserving the

computational properties of the Fast Fourier Transform (FFT) algorithm. Moreover, discretizing the spatial domain with trigonometric polynomials boundary conditions may be readily imposed [41, 42].

The paper is organized as follows. In Section 1 we present the evolutionary problem associated to the peridynamic Sine-Gordon equation and we prove the conservation of the associated energy. In Section 2 we propose a spectral discretization for the evolutionary problem and prove the convergence of the solutions of the semidiscretized problem to the ones of the continuous problem. In Section 3 the full discretization of the semi-discrete problem is obtained by using the Störmer-Verlet scheme. Section 4 is devoted to the numerical simulations: in Section 4.1 we firstly critically analyze strength and limitation of the proposed spectral method by validating the latter against a consolidated second-order finite difference scheme within several benchmark tests. Such tests include soliton-like solutions. Then, in Section 4.2 we demonstrate the presence of dispersive effects on the solution of the nonlocal evolutionary problem and, lastly, in Section 4.3 we experimentally prove the energy-preserving characteristic of the proposed spectral model. Conclusions and future outlines end the paper.

1. The model

We consider the nonlocal one-dimensional Sine-Gordon equation given by

$$\partial_{tt}^2 u(x, t) = \mathcal{L}u(x, t) - \sin(u(x, t)), \quad (1.1)$$

defined on a compact domain $\Omega \subset \mathbb{R}$, where \mathcal{L} is the integro-differential operator defined as

$$\mathcal{L}u(x, t) = \int_{B_\delta(x)} \frac{u(x, t) - u(x', t)}{|x - x'|^{1+2\alpha}} dx', \quad \alpha \in (0, 1), \quad (1.2)$$

where $B_\delta(x)$ is the x -centered ball with radius $\delta > 0$, with initial conditions

$$u(x, 0) = u_0(x), \quad \partial_t u(x, 0) = v_0(x). \quad (1.3)$$

The well-posedness of the Cauchy problem (1.1)-(1.3) in the energy space and in the framework of hyper-elastic constitutive assumptions can be found in [46]. Therein it is also showed that the energy associated to (1.1) is given by

$$\begin{aligned} E[u](t) = & \frac{1}{2} \int_{\Omega} |\partial_t u(x, t)|^2 dx - \frac{1}{4} \int_{\Omega} \int_{B_\delta(x)} \frac{(u(x, t) - u(x', t))^2}{|x - x'|^{1+2\alpha}} dx' dx \\ & - \int_{\Omega} (1 - \cos(u(x, t))) dx \end{aligned} \quad (1.4)$$

Lemma 1.1 (Energy preserving property). *The energy's functional defined in (1.4) is preserved by time.*

Proof. We have

$$\begin{aligned}
\frac{d}{dt}E[u](t) &= \int_{\Omega} \partial_t u(x, t) \partial_{tt}^2 u(x, t) dx \\
&\quad - \frac{1}{2} \int_{\Omega} \int_{B_{\delta}(x)} \frac{(u(x, t) - u(x', t))}{|x - x'|^{1+2\alpha}} (\partial_t u(x, t) - \partial_t u(x', t)) dx' dx \\
&\quad + \int_{\Omega} \partial_t u(x, t) \sin(u(x, t)) dx \\
&= \underbrace{\int_{\Omega} \partial_t u(x, t) (\partial_{tt}^2 u(x, t) + \sin(u(x, t))) dx}_{=: I_1} \\
&\quad - \frac{1}{2} \underbrace{\int_{\Omega} \int_{B_{\delta}(x)} \frac{(u(x, t) - u(x', t))}{|x - x'|^{1+2\alpha}} \partial_t u(x, t) dx' dx}_{=: I_2} \\
&\quad + \frac{1}{2} \underbrace{\int_{\Omega} \int_{B_{\delta}(x)} \frac{(u(x, t) - u(x', t))}{|x - x'|^{1+2\alpha}} \partial_t u(x', t) dx' dx}_{=: I_3}.
\end{aligned} \tag{1.5}$$

We need to show that $I_3 = -I_2$. If we use the constitutive assumptions on the pair-wise force interaction function, by making a change of variables and rearranging terms in I_3 we find

$$\begin{aligned}
I_3 &= \frac{1}{2} \int_{\Omega} \int_{B_{\delta}(0)} \frac{u(x, t) - u(x - x', t)}{|x'|^{1+2\alpha}} \partial_t u(x - x', t) dx' dx \\
&= \frac{1}{2} \int_{\Omega} \int_{B_{\delta}(0)} \frac{u(x, t) - u(x + x', t)}{|x'|^{1+2\alpha}} \partial_t u(x + x', t) dx' dx \\
&= -\frac{1}{2} \int_{\Omega} \int_{B_{\delta}(0)} \frac{u(x + x', t) - u(x, t)}{|x'|^{1+2\alpha}} \partial_t u(x + x', t) dx' dx \tag{1.6} \\
&= -\frac{1}{2} \int_{\Omega} \int_{B_{\delta}(x)} \frac{u(x, t) - u(x', t)}{|x - x'|^{1+2\alpha}} \partial_t u(x, t) dx' dx \\
&= -I_2.
\end{aligned}$$

Sustituting (1.6) into (1.5) and using (1.1) and the definition of the integral operator \mathcal{L} in (1.2), we get the claim. \square

2. Spectral semi-discretization

Pseudo-spectral methods are often used to study nonlinear wave phenomena [47]. They are based on the implementation of the fast-Fourier transform on equidistant collocation points and require the imposition of periodic boundary conditions. A different approach allowing to overcome the limitation of such boundary condition consists in considering the Chebyshev polynomials and the derivative matrix. Following this strategy, the nonlocal Sine-Gordon equation (1.1) can be discretized in space by using Chebyshev polynomials. The use of spectral methods allows us to obtain high accuracy in the profile of the solution and, moreover, this approach is typically used when the integral operator can be expressed in terms of convolution products [42, 41, 43]. Indeed, Chebyshev method can exploit the properties of the FFT algorithm to compute efficiently such products. Additionally, the choice of Chebyshev polynomials within the family of trigonometric polynomials allows us to impose more general boundary conditions.

The method consists in the approximation of the solution $u(x, t)$ to (1.1) by a finite linear combination of Chebyshev polynomials of the first kind.

For simplicity we assume the spatial domain to be $[-1, 1]$, but a more general spatial interval can be considered by an affine transformation. Moreover we assume to have no-flux boundary conditions

$$\partial_x u(\pm 1, t) = 0. \quad (2.1)$$

We derive the semi-discrete model of (1.1) as follows.

Let $N > 0$ be the total number of discretization points in the spatial domain $\Omega = [-1, 1]$ and $x_h = \cos(\pi h/N)$, $h = 0, \dots, N$ be the Chebyshev Gauss-Lobatto (CGL) points. We also define $\Omega_x = B_\delta(x) \cap [-1, 1]$, for any $x \in [-1, 1]$, so that $\Omega_0 = B_\delta(0) \cap [-1, 1]$.

Then, if we set

$$k(x) = \frac{1}{|x|^{1+2\alpha}} \chi_{\Omega_0}(x), \quad (2.2)$$

where χ_Ω denotes the characteristic function which takes value 1 if $x \in \Omega$ and value 0 otherwise, then we can rewrite equation (1.1) as follows

$$\partial_{tt}^2 u(x, t) = \beta u(x, t) - (k * u)(x, t) - \sin(u(x, t)), \quad (2.3)$$

where $\beta = \int_{B_\delta(0)} k(s) ds$.

We notice that β is well-defined because due to the nonlocal nature of the model, it does not allow self-interactions among material points and as a consequence the integrand k is not discontinuous over the domain of integration. Hence, we can assume that the kernel k is uniformly bounded.

We look for an approximation of the solution $u(x, t)$ in the form of a finite linear combination of Chebyshev polynomials $T_n(x)$

$$u^N(x, t) = \sum_{n=0}^N \tilde{u}_n(t) T_n(x), \quad x \in \Omega, \quad t > 0, \quad (2.4)$$

where the coefficients $\tilde{u}_n(t)$ represent the discrete Chebyshev coefficients

given by

$$\tilde{u}_n = \frac{1}{\gamma_n} \sum_{h=0}^N u(x_h) T_n(x_h) w_h, \quad (2.5)$$

where γ_n is a normalization constant defined by

$$\gamma_n = \begin{cases} \pi & n = 0, N \\ \frac{\pi}{2} & n = 1, \dots, N-1 \end{cases} \quad (2.6)$$

and

$$w_h = \begin{cases} \frac{\pi}{2N} & h = 0, N \\ \frac{\pi}{N} & h = 1, \dots, N-1. \end{cases} \quad (2.7)$$

The presence of these constants is required to ensure the orthogonality property of the Chebyshev polynomials with respect to the weight function $w(x) = 1/\sqrt{1-x^2}$.

We substitute u by u^N into (2.3). Since Chebyshev transform, denoted here by \mathcal{F} , fulfills the same properties of Fourier transform, we can rewrite a convolution product in the physic space as a multiplication of the Chebyshev transform of each factor in the frequency space. Thus, on each interior collocation point x_h , $h = 1, \dots, N-1$, equation (2.3) can be approximated as follows

$$\partial_{tt}^2 u^N(x_h, t) = \beta u^N(x_h, t) - \mathcal{F}^{-1}(\mathcal{F}(k) \mathcal{F}(u^N))(x_h, t) - \sin(u^N(x_h, t)). \quad (2.8)$$

In the same way we approximate the initial conditions in (1.3) by

$$u^N(x_h, 0) = u_0(x_h), \quad \partial_t u^N(x_h, 0) = v_0(x_h), \quad h = 0, \dots, N. \quad (2.9)$$

Following [48], in order to impose Neumann boundary conditions to the discrete approximated solution

$$\partial_x u^N(x_0, t) = \partial_x u^N(x_N) = 0, \quad (2.10)$$

on each time level we have to solve the 2×2 system

$$\begin{cases} d_{00}u^N(x_0, t) + d_{0N}u^N(x_N, t) &= -\sum_{h=1}^{N-1} d_{0h}u^N(x_h, t), \\ d_{NN}u^N(x_N, t) + d_{N0}u^N(x_0, t) &= -\sum_{h=1}^{N-1} d_{Nh}u^N(x_h, t), \end{cases} \quad (2.11)$$

where $D = (d_{ij})$, $i, j = 0, \dots, N$ is the matrix representing the spectral derivative at the CGL collocation points (an explicit formula for the component of D can be found in [49]). For readers' convenience, we remark that equations (2.11) basically represent the multiplication of the first row and the last row of the derivative matrix D by u^N . Indeed, the left-hand side refers to the derivative of u^N at the boundary meshpoints x_0 and x_N .

We can prove the convergence of the semi-discrete scheme (2.8)-(2.9)-(2.10) in the framework of weighted Sobolev space $H_w^s(\Omega)$, $s \geq 1$.

We start by introducing the functional setting under consideration. In what follows, C denotes a generic positive constant. We denote by $(\cdot, \cdot)_w$ and $\|\cdot\|_w$ the inner product and the norm of $L_w^2(\Omega)$, respectively, namely

$$(u, v)_w = \int_{\Omega} u(x)v(x)w(x) dx, \quad \|u\|_w^2 = (u, u)_w,$$

with $w(x) = \left(\sqrt{1-x^2}\right)^{-1}$.

Let $s > 0$, $H_w^s(\Omega)$ be the weighted Sobolev space and $X_s = C^1(0, T; H_w^s(\Omega))$

be the space of all continuous functions in $H_w^s(\Omega)$ whose distributional derivative is in $H_w^s(\Omega)$, with norm

$$\|u\|_{X_s}^2 = \max_{t \in [0, T]} \left(\|u(\cdot, t)\|_w^2 + \|\partial_t u(\cdot, t)\|_w^2 \right),$$

for any $T > 0$.

We introduce the space of Chebyshev polynomials of degree N as follows

$$S_N = \text{span} \{T_k(x) \mid -N \leq k \leq N\},$$

and we define the projection operator $P_N : L_w^2(\Omega) \rightarrow S_N$ as

$$P_N u(x) = \sum_{|k| \leq N} \tilde{u}_k T_k(x).$$

It is such that for any $u \in L_w^2(\Omega)$, the following equality holds

$$(u - P_N u, \varphi)_w = 0, \quad \text{for every } \varphi \in S_N. \quad (2.12)$$

We have that the projector operator P_N commutes with derivatives in the distributional sense:

$$\partial_x^q P_N u = P_N \partial_x^q u, \quad \text{and} \quad \partial_t^q P_N u = P_N \partial_t^q u.$$

Then, spectral scheme (2.8)-(2.9)-(2.10) can be rewritten by using the

projection P_N in the following way

$$\begin{aligned}\partial_{tt}^2 u^N &= P_N \mathcal{L}(u^N) - P_N \sin(u^N), \\ u^N(x, 0) &= P_N u_0(x), \quad \partial_t u^N(x, 0) = P_N v(x), \\ \partial_x u^N(\pm 1, t) &= 0,\end{aligned}\tag{2.13}$$

where $u^N(x, t) \in S_N$ for every $0 \leq t \leq T$.

We recall the following lemma which is preliminary to our result.

Lemma 2.1 (see [50]). *Let $0 \leq \mu \leq s$, if $u \in H_w^s(\Omega)$, then the following inequality holds*

$$\|u - P_N u\|_{H_w^\mu(\Omega)} \leq C N^{\mu-s} \|u\|_{H_w^s(\Omega)},\tag{2.14}$$

for any positive constant C .

We can prove the following theorem.

Theorem 2.2. *Let $s \geq 1$, and assume $u(x, t) \in X_s$ is the solution of the problem (1.1) with initial conditions $u_0, v \in H_w^s(\Omega)$, and $u^N(x, t)$ is the solution of the semi-discrete scheme (2.13). Then, there exists a positive constant $C = C(T)$, which does not depend on N , such that*

$$\|u - u^N\|_{X_1} \leq CL(T) \left(\frac{1}{N}\right)^{s-1} \|u\|_{X_s}.\tag{2.15}$$

Proof. Let $s \geq 1$. Triangular inequality gives us

$$\|u - u^N\|_{X_1} \leq \|u - P_N u\|_{X_1} + \|P_N u - u^N\|_{X_1}.\tag{2.16}$$

Let we first focus on $\|u - P_N u\|_{X_1}$. Thanks to Lemma 2.1 we have

$$\|(u - P_N u)(\cdot, t)\|_{H_w^1(\Omega)} \leq C N^{1-s} \|u(\cdot, t)\|_{H_w^s(\Omega)},$$

and

$$\|\partial_t(u - P_N u)(\cdot, t)\|_{H_w^1(\Omega)} \leq C N^{1-s} \|\partial_t u(\cdot, t)\|_{H_w^s(\Omega)}.$$

Therefore,

$$\|u - P_N u\|_{X_1} \leq C N^{1-s} \|u\|_{X_s}. \quad (2.17)$$

We now estimate the term $\|P_N u - u^N\|_{X_1}$. We fix $\varphi = \partial_t(P_N u - u^N) \in S_N$ as test function. Subtracting (2.13) from (1.1) and taking the inner product with the test function φ , we get

$$\begin{aligned} 0 &= \underbrace{\int_{\Omega} (\partial_{tt}^2 u(x, t) - \partial_{tt}^2 u^N(x, t)) \partial_t (P_N u(x, t) - u^N(x, t)) w(x) dx}_{=: I_1} \\ &\quad - \underbrace{\int_{\Omega} (\mathcal{L}(u(x, t)) - P_N \mathcal{L}(u^N(x, t))) \partial_t (P_N u(x, t) - u^N(x, t)) w(x) dx}_{=: I_2} \\ &\quad + \underbrace{\int_{\Omega} (\sin(u(x, t)) - P_N \sin(u^N(x, t))) \partial_t (P_N u(x, t) - u^N(x, t)) w(x) dx}_{=: I_3}. \end{aligned} \quad (2.18)$$

We focus on I_1 . The orthogonal condition (2.12) implies that

$$\int_{\Omega} (\partial_{tt}^2 u(x, t) - P_N \partial_{tt}^2 u(x, t)) \partial_t (P_N u(x, t) - u^N(x, t)) w(x) dx = 0.$$

Thus,

$$\begin{aligned}
I_1 &= \int_{\Omega} (\partial_{tt}^2 u(x, t) - P_N \partial_{tt}^2 u(x, t)) \partial_t (P_N u(x, t) - u^N(x, t)) w(x) dx \\
&\quad + \int_{\Omega} (P_N \partial_{tt}^2 u(x, t) - \partial_{tt}^2 u^N(x, t)) \partial_t (P_N u(x, t) - u^N(x, t)) w(x) dx \\
&= \frac{1}{2} \frac{d}{dt} \|\partial_t (P_N u - u^N)(\cdot, t)\|_{H_w^1(\Omega)}^2.
\end{aligned} \tag{2.19}$$

Thanks to (2.12), we have

$$\int_{\Omega} (\mathcal{L}(u^N(x, t)) - P_N \mathcal{L}(u^N(x, t))) \partial_t (P_N u(x, t) - u^N(x, t)) w(x) dx = 0.$$

Thus, since $k \in L^\infty(\Omega)$, using the Cauchy's inequality, we have

$$\begin{aligned}
I_2 &= \int_{\Omega} (\mathcal{L}(u(x, t)) - \mathcal{L}(u^N(x, t))) \partial_t (P_N u(x, t) - u^N(x, t)) w(x) dx \\
&= \int_{\Omega} \int_{\Omega_x} k(x' - x) (u(x', t) - u(x, t)) \partial_t (P_N u(x, t) - u^N(x, t)) w(x) dx' dx \\
&\quad - \int_{\Omega} \int_{\Omega_x} k(x' - x) (u^N(x', t) - u^N(x, t)) \partial_t (P_N u(x, t) - u^N(x, t)) w(x) dx' dx \\
&\leq \int_{\Omega} \int_{\Omega_x} k(x' - x) |u(x', t) - u^N(x', t)| \partial_t (P_N u(x, t) - u^N(x, t)) w(x) dx' dx \\
&\quad + \int_{\Omega} \int_{\Omega_x} k(x' - x) |u(x, t) - u^N(x, t)| \partial_t (P_N u(x, t) - u^N(x, t)) w(x) dx' dx \\
&\leq \left(\frac{\beta}{2} + \|k\|_{L^\infty(\Omega)} \right) \left(\|(u - u^N)(\cdot, t)\|_{H_w^1(\Omega)}^2 + \|\partial_t (P_N u - u^N)(\cdot, t)\|_{H_w^1(\Omega)}^2 \right).
\end{aligned} \tag{2.20}$$

Moreover, the orthogonality condition (2.12) ensures that

$$\int_{\Omega} (\sin(u^N(x, t)) - P_N \sin(u^N(x, t))) \partial_t (P_N u(x, t) - u^N(x, t)) w(x) dx = 0.$$

Therefore, due to the uniformly Lipschitzianity of the loading term and the Cauchy's inequality, we find

$$\begin{aligned}
I_3 &= \int_{\Omega} (\sin(u(x, t)) - P_N \sin(u^N(x, t))) \partial_t (P_N u(x, t) - u^N(x, t)) w(x) dx \\
&= \int_{\Omega} (\sin(u(x, t)) - \sin(u^N(x, t))) \partial_t (P_N u(x, t) - u^N(x, t)) w(x) dx \\
&\leq \frac{1}{2} \left(\| (u - u^N)(\cdot, t) \|_{H_w^1(\Omega)}^2 + \| \partial_t (P_N u - u^N)(\cdot, t) \|_{H_w^1(\Omega)}^2 \right).
\end{aligned} \tag{2.21}$$

We substitute (2.19), (2.20) and (2.21) in (2.18) and we obtain

$$\frac{1}{2} \frac{d}{dt} \| \partial_t (P_N u - u^N)(\cdot, t) \|_{H_w^1(\Omega)}^2 \leq C \| (u - u^N)(\cdot, t) \|_{H_w^1(\Omega)}^2 + C \| \partial_t (P_N u - u^N)(\cdot, t) \|_{H_w^1(\Omega)}^2. \tag{2.22}$$

We add to both sides of equation (2.22) the term

$$\frac{1}{2} \frac{d}{dt} \| (P_N u - u^N)(\cdot, t) \|_{H_w^1(\Omega)}^2 = \int_{\Omega} (P_N u(x, t) - u^N(x, t)) \partial_t (P_N u(x, t) - u^N(x, t)) w(x) dx,$$

then, we find

$$\begin{aligned}
&\frac{d}{dt} \left(\| \partial_t (P_N u - u^N)(\cdot, t) \|_{H_w^1(\Omega)}^2 + \| (P_N u - u^N)(\cdot, t) \|_{H_w^1(\Omega)}^2 \right) \\
&\leq C \left(\| \partial_t (P_N u - u^N)(\cdot, t) \|_{H_w^1(\Omega)}^2 + \| (P_N u - u^N)(\cdot, t) \|_{H_w^1(\Omega)}^2 + \| (u - P_N u)(\cdot, t) \|_{H_w^1(\Omega)}^2 \right).
\end{aligned}$$

Since $\| \partial_t (P_N u - u^N)(\cdot, 0) \|_{H_w^1(\Omega)} = 0$ and $\| (P_N u - u^N)(\cdot, 0) \|_{H_w^1(\Omega)} = 0$,

we can apply Lemma 2.1 and Gronwall's inequality obtaining

$$\left(\| \partial_t (P_N u - u^N)(\cdot, t) \|_{H_w^1(\Omega)}^2 + \| (P_N u - u^N)(\cdot, t) \|_{H_w^1(\Omega)}^2 \right)$$

$$\begin{aligned}
&\leq \int_0^t e^{C(t-\tau)} \|(u - P_N u)(\cdot, \tau)\|_{H_w^1(\Omega)}^2 d\tau \\
&\leq C(T) N^{2-2s} \int_0^t \|u(\cdot, \tau)\|_{H_w^1(\Omega)}^2 d\tau.
\end{aligned}$$

Hence,

$$\|P_N u - u^N\|_{X_1} \leq C(T) N^{1-s} \|u\|_{X_s}. \quad (2.23)$$

Finally, using (2.17) and (2.23) in (2.16), we get the claim. \square

3. The fully discrete scheme

The semi-discrete nonlocal formulation of Sine-Gordon equation in (2.8) can be integrated in time by using explicit forward and backward difference techniques.

Störmer-Verlet method consists in a centered second-order finite difference scheme deeply used in the context of continuum mechanics and elastodynamics as it is an energy-preserving scheme due to its symplectic nature (see for instance [51]).

$N_T > 0$ be the total number of time steps and $\{t_s\}_{s=0}^{N_T}$ be a uniform partition of the computational interval $[0, T]$, with $t_s = s\Delta t$ and $\Delta t = \frac{T}{N_T}$.

If we denote by

$$\mathcal{L}(u^N(\cdot, t))(x_h) = \beta u^N(x_h, t) - \mathcal{F}^{-1}(\mathcal{F}(k)\mathcal{F}(u^N))(x_h, t) \quad (3.1)$$

the spectral discretization of the nonlocal operator \mathcal{L} at the collocation points x_h , $h = 0, \dots, N$, then the semi-discrete scheme (2.8) can be com-

pactly written as

$$\partial_{tt}^2 u^N(x_h, t) = \mathcal{L}(u^N(x_h, t)) - \sin(u^N(x_h, t)), \quad h = 0, \dots, N. \quad (3.2)$$

We set $U_h^{N,s} = u^N(x_h, t_s)$ the approximation of the solution at the node x_h and at the discrete time t_s , for $h = 0, \dots, N$ and $s = 0, \dots, N_T$ and we denote $V_h^{N,s} = (U_h^{N,s})'$, then the Störmer-Verlet scheme for the system (3.2) is given by

$$\begin{cases} U_h^{N,s+1} = U_h^{N,s} + \Delta t \left(V_h^{N,s} + \frac{\Delta t}{2} \mathcal{L}(U_h^{N,s}) - \frac{\Delta t}{2} \sin(U_h^{N,s}) \right), \\ V_h^{N,s+1} = V_h^{N,s} + \frac{\Delta t}{2} \left(\mathcal{L}(U_h^{N,s}) - \sin(U_h^{N,s}) + \mathcal{L}(U_h^{N,s+1}) - \sin(U_h^{N,s+1}) \right), \end{cases} \quad (3.3)$$

for $h = 0, \dots, N$ and $s = 0, \dots, N_T$.

4. Numerical experiments

In this section we perform several simulations in order to study the properties of the solution of the model. The first test provides a validation of the spectral method by making a comparison between the solution obtained by Chebyshev method with the solution obtained by implementing a centered second order finite difference scheme. Then we show the dispersive effects due to the nonlocality in the profile of soliton-type solutions. Finally, we point out the energy-preserving property.

4.1. Test 1: Validation of the performance of the spectral method

In order to show that the spectral method approximates the correct solution, we make a comparison between the solution provided by the pro-

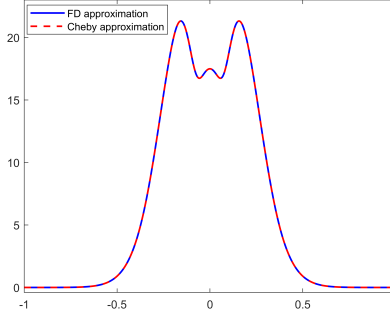


Figure 1: With reference to Section 4.1, the comparison between the approximated solution computed by spectral method with the one obtained by finite different discretization at time $t = 1$ with initial conditions $u_{0,1}(x)$ and $v_{0,1}(x)$. The parameters for the simulation are $N = 400$, $N_T = 800$, the horizon is $\delta = 0.2$ and $\alpha = 0.4$.

posed Chebyshev method and the solution found by the implementation of a finite difference discretization. The latter corresponding to a centered second-ordered scheme in time explicitly combined with the trapezoidal rule approximation of the operator $\mathcal{L}u(x, t)$. We choose $u_{0,1}(x) = 0$ and $v_{0,1}(x) = 4 \left(\sqrt{1 - c^2} \cosh(x/\sqrt{1 - c^2}) \right)^{-1}$ as initial conditions, with $c = 0.999$. We fix $\alpha = 0.4$ as parameter of the integral operator \mathcal{L} defined in (0.4) and $\delta = 0.2$ as horizon. In Figure 1, we can observe a good agreement between the two numerical solutions.

In Figure 2 we show the comparison between the solution obtained by spectral method and finite difference method corresponding to the initial conditions $u_{0,2}(x) = 4 \arctan \left(e^{\frac{x}{\sqrt{1 - c^2}}} \right)$ and $v_{0,2}(x) = -2c \frac{\text{sech} \left(\frac{x}{\sqrt{1 - c^2}} \right)}{\sqrt{1 - c^2}}$, with $c = 0.999$.

With reference to the solution corresponding to the initial conditions $u_{0,2}(x)$ and $v_{0,2}(x)$, we also provide a convergence analysis of the proposed

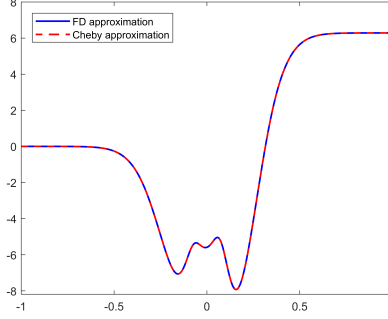


Figure 2: With reference to Section 4.1, the comparison between the approximated solution computed by spectral method with the one obtained by finite different discretization at time $t = 1$ with initial conditions $u_{0,2}(x)$ and $v_{0,2}(x)$. The parameters for the simulation are $N = 400$, $\Delta t = 8/N_T$, $N_T = 800$ $\delta = 0.2$ and $\alpha = 0.4$.

spectral scheme. We define the relative L^2 -error as follows

$$Error_2 [u^N] (t) = \frac{\sum_{h=1}^N |u^N(x_h, t) - u^*(x_h, t)|^2}{\sum_{h=1}^N |u^*(x_h, t)|^2},$$

where u^* represents the reference solution obtained by using the finite difference scheme with $N = 1600$. Starting from the relative L^2 -error, we can compute the convergence rate by looking for the slope of the line that best fit in the sense of least square the logarithm of the data.

Table 1 and Figure 3 depict the relative L^2 -error and the convergence rate obtained by using the finite difference scheme and the proposed spectral method as the total number of spatial discretization points increases.

We can observe a gain in terms of convergence rate when a spectral method is applied.

N	Finite Difference method		Chebyshev method	
	error	conv. rate	error	conv. rate
100	2.1336×10^{-3}	—	1.3600×10^{-3}	—
200	4.7141×10^{-4}	2.1625	1.9584×10^{-4}	27757
400	1.0768×10^{-4}	2.1426	7.1261×10^{-6}	3.7670
800	1.8644×10^{-5}	2.2551	3.8717×10^{-7}	3.9945

Table 1: With reference to Section 4.1, the relative error related to the initial conditions $u_{0,2}(x)$ and $v_{0,2}(x)$, at time $t = 2$ as function of the total number of discretization points.

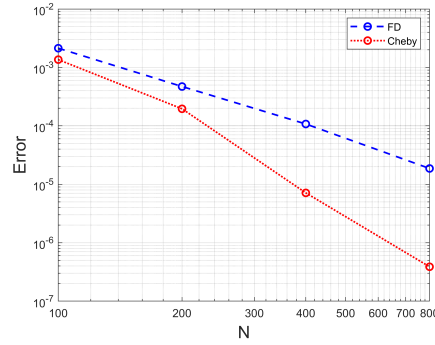


Figure 3: With reference to Section 4.1, the comparison between the relative error obtained with the two considered methods in the logarithmic scale.

4.2. Test 2: The dispersive effects of the nonlocal model in soliton-type solutions

Due to the presence of long-range interactions, solutions of (1.1) are characterized by a dispersive behavior. As a consequence, soliton-type solutions lose the property to be travelling waves with constant velocity and shape-preserving profile and show the appearance of an oscillatory behavior, whose phase depends on the size of the horizon.

The nonlocal kink solution is compared with the classical one in Figure 4, where we can observe the evolution of the solution subject to the following initial conditions

$$\begin{aligned} u_0(x) &= 4 \arctan \left(e^{\frac{x}{\sqrt{1-c^2}}} \right), \\ v_0(x) &= -2c \frac{\operatorname{sech} \left(\frac{x}{\sqrt{1-c^2}} \right)}{\sqrt{1-c^2}}, \end{aligned}$$

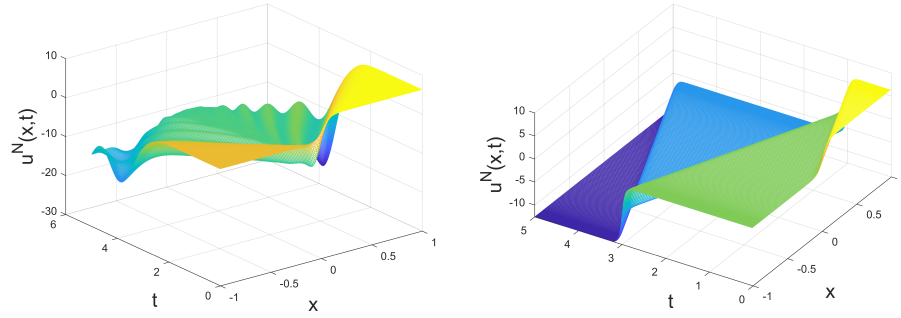
with velocity $c = .999$.

A comparison between antikink solutions is shown in Figure 5. The initial conditions for this test are

$$\begin{aligned} u_0(x) &= 4 \arctan \left(e^{\frac{-x}{\sqrt{1-c^2}}} \right), \\ v_0(x) &= -2c \frac{\operatorname{sech} \left(\frac{x}{\sqrt{1-c^2}} \right)}{\sqrt{1-c^2}}, \end{aligned}$$

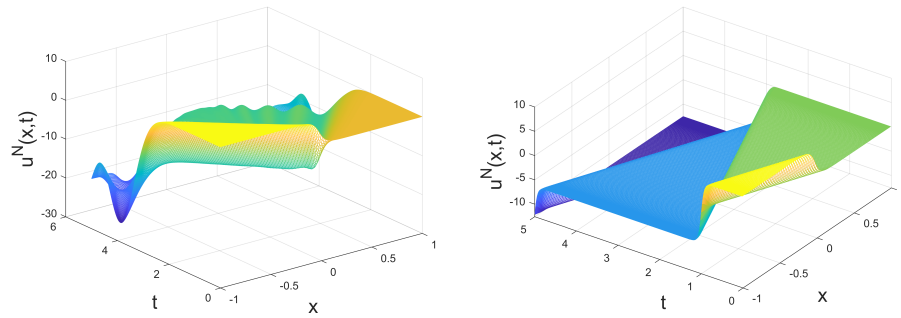
with $c = 0.999$.

Figures 6 and 7 provide a comparison between local and nonlocal models in the case of a collision between two kink-type solitons or a collision between



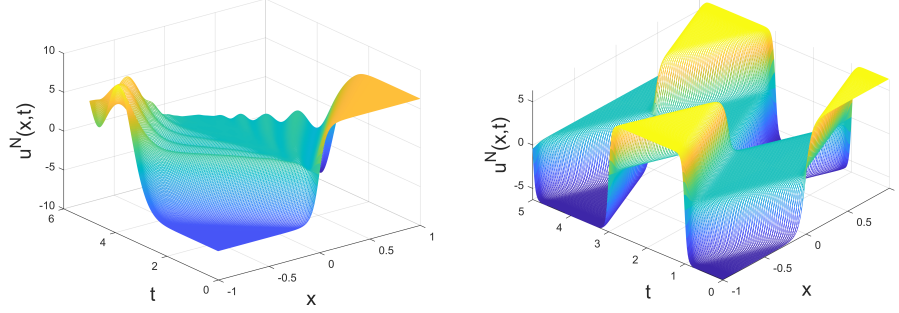
The evolution of a kink soliton in the nonlocal model. The evolution of a kink soliton in the classical Sine-Gordon equation.

Figure 4: With reference to Section 4.2: the comparison between kink-type solitons in the nonlocal model and in the classical Sine-Gordon model. The parameters for the simulation are $\delta = 0.2$, $N = 200$, $\alpha = 0.4$, and $N_T = 400$.



The evolution of an antikink soliton in the nonlocal model. The evolution of an antikink soliton in the classical Sine-Gordon equation.

Figure 5: With reference to Section 4.2: the comparison between antikink-type solitons in the nonlocal model and in the classical Sine-Gordon model. The parameters for the simulation are $\delta = 0.2$, $N = 200$, $\alpha = 0.4$, and $\Delta t = 8/N_T$, $N_T = 400$.



The evolution of a collision of two kink solitons in the nonlocal model. The evolution of a collision of two kink solitons in the classical Sine-Gordon equation.

Figure 6: With reference to Section 4.2: the comparison between the behavior of a collision of two kink-type solitons in the nonlocal model and in the classical Sine-Gordon model. The parameters for the simulation are $\delta = 0.2$, $N = 200$, $\alpha = 0.4$, and $\Delta t = 8/N_T$, $N_T = 400$.

a kink and an antikink soliton, respectively. The initial conditions for these simulations are respectively

$$u_0(x) = 4 \arctan \left(c \sinh \frac{x}{\sqrt{1-c^2}} \right),$$

$$v_0(x) = 0,$$

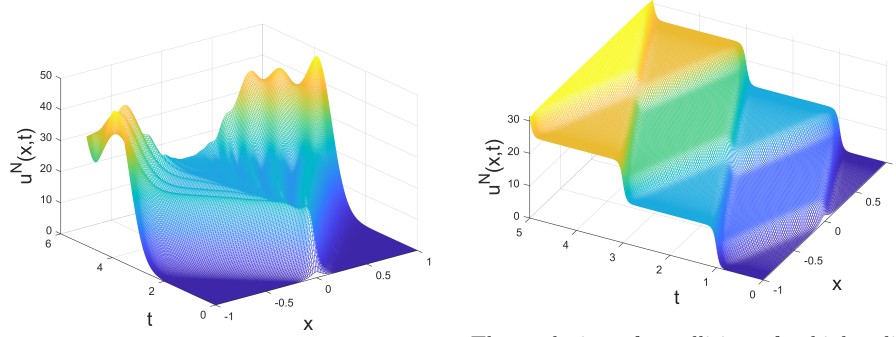
and

$$u_0(x) = 0,$$

$$v_0(x) = \frac{4}{\sqrt{1-c^2} \cosh \left(\frac{x}{\sqrt{1-c^2}} \right)},$$

with $c = 0.999$.

Finally, the same dispersive effects can be observed even in the behavior of a breather solution as shown in Figure 8. In this case the initial conditions



The evolution of a collision of a kink soliton with an antikink soliton in the nonlocal model. Gordon equation.

Figure 7: With reference to Section 4.2: the comparison between the behavior of a collision of kink-type soliton with an antikink-type soliton in the nonlocal model and in the classical Sine-Gordon model. The parameters for the simulation are $\delta = 0.2$, $N = 200$, $\alpha = 0.4$, and $\Delta t = 8/N_T$, $N_T = 400$.

for the simulation are

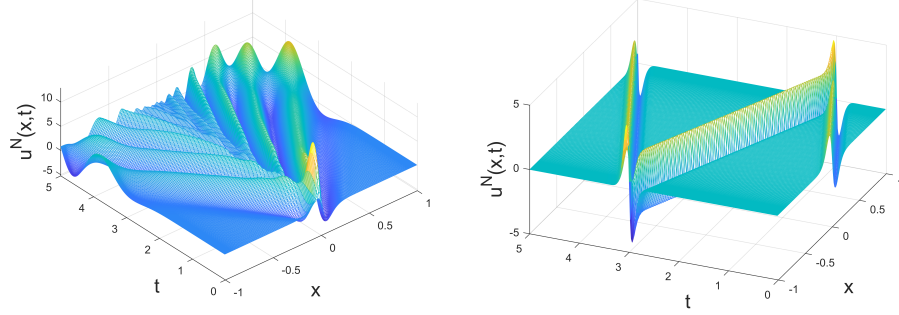
$$u_0(x) = 4 \arctan \left(\frac{\sqrt{1-w^2} \sin \left(-\frac{cwx}{\sqrt{1-c^2}} \right)}{w \cosh \left(\frac{x\sqrt{1-w^2}}{\sqrt{1-c^2}} \right)} \right),$$

$$v_0(x) = 4w \frac{\sqrt{1-w^2}}{\sqrt{1-c^2}} \left(\frac{w \cos \left(-\frac{cwx}{\sqrt{1-c^2}} \right) \cosh \left(\frac{x\sqrt{1-w^2}}{\sqrt{1-c^2}} \right) + c\sqrt{1-w^2} \sin \left(-\frac{cwx}{\sqrt{1-c^2}} \right) \sinh \left(\frac{x\sqrt{1-w^2}}{\sqrt{1-c^2}} \right)}{w^2 \cosh^2 \left(\frac{x\sqrt{1-w^2}}{\sqrt{1-c^2}} \right) + (1-w^2) \sin^2 \left(-\frac{cwx}{\sqrt{1-c^2}} \right)} \right),$$

with $c = 0.999$ and $w = 0.4$. In all shown cases, due to the dispersive effects, we can also observe a time delay in the soliton waves to reach the boundaries with respect to the local soliton waves.

4.3. Test 3: The energy-preserving properties of the solution

As mentioned in Section 3, we show the energy-preserving property of the proposed numerical scheme. We consider $u_0(x) = e^{-x^2/1002}$, $v_0(x) = 0$, $\delta = 0.2$, $\alpha = 0.4$ and we fix $N = 800$ and $\Delta t = 10^{-4}$. We compute the



The evolution of a breather soliton in the non- The evolution of a breather soliton in the clas-
local model. sical Sine-Gordon equation.

Figure 8: With reference to Section 4.2: the comparison between the behavior of a breather-type soliton in the nonlocal model and in the classical Sine-Gordon model. The parameters for the simulation are $\delta = 0.2$, $N = 200$, $\alpha = 0.4$, and $\Delta t = 8/N_T$, $N_T = 400$.

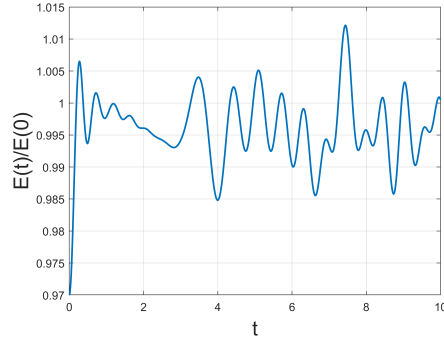


Figure 9: With reference to Section 4.3, the conservation of the energy's functional.

energy functional associated with the spectral solution having $u_0(x)$ and $v_0(x)$ as initial conditions by using (1.4).

Figure 9 shows that the energy functional $E(t)/E(0)$ oscillates around a constant value.

Conclusive Remarks

A spectral method based on the Chebyshev nodes spatial discretization for the Cauchy problem related to the evolution of the peridynamic Sine-Gordon equation has been studied in this work. The consistency of such discretization has been rigorously proved and various numerical experiments have clarified strength and limitations of the proposed model. Specifically, the proposed model has been validated against a second order centered finite-difference scheme by comparing the evolution in time of several nonlocal soliton-type solutions. Lastly, dispersive effects as well as the ability of preserving the internal energy of the specific peridynamic kernel have been experimentally and theoretically demonstrated.

Acknowledgments

AC, LL, and SFP are members of Gruppo Nazionale per il Calcolo Scientifico (GNCS) of the Istituto Nazionale di Alta Matematica (INdAM). This work was partially supported by:

- Research Project of National Relevance “Evolution problems involving interacting scales” granted by the Italian Ministry of Education, University and Research (MUR Prin 2022, project code 2022M9BKBC, Grant No. CUP D53D23005880006);
- Research Project of National Relevance “Mathematical Modeling of Biodiversity in the Mediterranean sea: from bacteria to predators, from meadows to currents” granted by the Italian Ministry of University and Research (MUR) under the National Recovery and Resilience

Plan (NRRP) funded by the European Union - NextGenerationEU
(MUR Prin PNRR 2023, project code P202254HT8, Grant No. CUP
B53D23027760001);

- PNRR MUR - M4C2 Project, grant number N00000013 - CUP D93C22000430001;
- the INdAM-GNCS Project CUP - E53C23001670001.

References

- [1] N. Asano, Y. Kato, Algebraic and spectral methods for nonlinear wave equations, volume 49, Longman Scientific and Technical, 1990.
- [2] M. J. Ablowitz, H. Segur, Solitons and the inverse scattering transform, SIAM, 1981.
- [3] Z.-f. Liang, X.-y. Tang, W. Ding, Infinitely many nonlocal symmetries and nonlocal conservation laws of the integrable modified kdv-sine-gordon equation, Communications in Theoretical Physics 73 (2021) 055003.
- [4] G. Wang, A novel $(3+1)$ -dimensional sine-gordon and a sinh-gordon equation: derivation, symmetries and conservation laws, Applied Mathematics Letters 113 (2021) 106768.
- [5] H. Blas, H. F. Callisaya, J. Campos, Riccati-type pseudo-potentials, conservation laws and solitons of deformed sine-gordon models, Nuclear Physics B 950 (2020) 114852.

- [6] P. Miškinis, The nonlinear and nonlocal integrable sine-gordon equation, *Mathematical Modelling and Analysis* 10 (2005) 367–376.
- [7] G. Alfimov, V. Eleonsky, L. Lerman, Solitary wave solutions of nonlocal sine-gordon equations, *Chaos: An Interdisciplinary Journal of Nonlinear Science* 8 (1998) 257–271.
- [8] J.-y. Wang, X.-y. Tang, Z.-f. Liang, S.-y. Lou, Infinitely many nonlocal symmetries and conservation laws for the $(1+1)$ -dimensional sine-gordon equation, *Journal of Mathematical Analysis and Applications* 421 (2015) 685–696.
- [9] G. Alfimov, T. Pierantozzi, L. Vázquez, Numerical study of a nonlocal sine-gordon equation, in: *Nonlinear Waves: Classical and Quantum Aspects*, Springer, 2005, pp. 121–128.
- [10] X.-y. Tang, Z.-f. Liang, J.-y. Wang, Nonlocal topological solitons of the sine-gordon equation, *Journal of Physics A: Mathematical and Theoretical* 48 (2015) 285204.
- [11] X.-b. Xiang, W. Feng, S.-l. Zhao, Local and nonlocal complex discrete sine-gordon equation. solutions and continuum limits, *Theoretical and Mathematical Physics* 211 (2022) 758–774.
- [12] S. A. Silling, Reformulation of elasticity theory for discontinuities and long-range forces, *J. Mech. Phys. Solids* 48 (2000) 175–209.
URL: [https://doi.org/10.1016/S0022-5096\(99\)00029-0](https://doi.org/10.1016/S0022-5096(99)00029-0). doi:10.1016/S0022-5096(99)00029-0.

- [13] S. A. Silling, Linearized theory of peridynamic states, *J. Elasticity* 99 (2010) 85–111. URL: <https://doi.org/10.1007/s10659-009-9234-0>. doi:10.1007/s10659-009-9234-0.
- [14] Q. Du, Y. Tao, X. Tian, A peridynamic model of fracture mechanics with bond-breaking, *J. Elasticity* 132 (2018) 197–218. URL: <https://doi.org/10.1007/s10659-017-9661-2>. doi:10.1007/s10659-017-9661-2.
- [15] E. Emmrich, D. Puhst, Measure-valued and weak solutions to the nonlinear peridynamic model in nonlocal elastodynamics, *Nonlinearity* 28 (2015) 285–307. URL: <https://doi.org/10.1088/0951-7715/28/1/285>. doi:10.1088/0951-7715/28/1/285.
- [16] A. C. Eringen, *Nonlocal continuum field theories*, Springer-Verlag, New York, 2002.
- [17] A. C. Eringen, D. G. B. Edelen, On nonlocal elasticity, *Internat. J. Engrg. Sci.* 10 (1972) 233–248. URL: [https://doi.org/10.1016/0020-7225\(72\)90039-0](https://doi.org/10.1016/0020-7225(72)90039-0). doi:10.1016/0020-7225(72)90039-0.
- [18] E. Kröner, Elasticity theory of materials with long range cohesive forces, *International Journal of Solids and Structures* 3 (1967) 731–742. URL: <https://www.sciencedirect.com/science/article/pii/0020768367900492>. doi:[https://doi.org/10.1016/0020-7683\(67\)90049-2](https://doi.org/10.1016/0020-7683(67)90049-2).
- [19] S. Silling, R. Lehoucq, Peridynamic theory of solid mechanics, in: H. Aref, E. van der Giessen (Eds.), *Advances in*

- Applied Mechanics, volume 44 of *Advances in Applied Mechanics*, Elsevier, 2010, pp. 73–168. URL: <https://www.sciencedirect.com/science/article/pii/S0065215610440028>. doi:[https://doi.org/10.1016/S0065-2156\(10\)44002-8](https://doi.org/10.1016/S0065-2156(10)44002-8).
- [20] S. A. Silling, Linearized theory of peridynamic states, *J. Elasticity* 99 (2010) 85–111. URL: <https://doi.org/10.1007/s10659-009-9234-0>. doi:10.1007/s10659-009-9234-0.
- [21] S. A. Silling, M. Epton, O. Weckner, J. Xu, E. Askari, Peridynamic states and constitutive modeling, *J. Elasticity* 88 (2007) 151–184. URL: <https://doi.org/10.1007/s10659-007-9125-1>. doi:10.1007/s10659-007-9125-1.
- [22] S. A. Silling, R. B. Lehoucq, Convergence of peridynamics to classical elasticity theory, *J. Elasticity* 93 (2008) 13–37. URL: <https://doi.org/10.1007/s10659-008-9163-3>. doi:10.1007/s10659-008-9163-3.
- [23] G. M. Coclite, S. Dipierro, G. Fanizza, F. Maddalena, M. Romano, E. Valdinoci, Qualitative aspects in nonlocal dynamics, *Journal of Peridynamics and Nonlocal Modeling* (2021). URL: <https://doi.org/10.1007/s42102-021-00064-z>. doi:10.1007/s42102-021-00064-z.
- [24] G. M. Coclite, S. Dipierro, G. Fanizza, F. Maddalena, E. Valdinoci, Dispersive effects in a scalar nonlocal wave equation inspired by peridynamics, *Nonlinearity* 35 (2022) 5664. URL: <https://dx.doi.org/10.1088/1361-6544/ac8fd9>. doi:10.1088/1361-6544/ac8fd9.

- [25] A. Coclite, G. M. Coclite, G. Fanizza, F. Maddalena, Dispersive effects in two- and three-dimensional peridynamics, *Acta Applicandae Mathematicae* 187 (2023) 13. URL: <https://doi.org/10.1007/s10440-023-00606-1>. doi:10.1007/s10440-023-00606-1.
- [26] R. Lipton, Dynamic brittle fracture as a small horizon limit of peridynamics, *Journal of Elasticity* 117 (2014) 21–50.
- [27] R. Lipton, Cohesive dynamics and brittle fracture, *Journal of Elasticity* 124 (2016) 143–191.
- [28] P. K. Jha, R. Lipton, Numerical analysis of nonlocal fracture models in hölder space, *SIAM Journal on Numerical Analysis* 56 (2018) 906–941. URL: <https://doi.org/10.1137/17M1112236>. doi:10.1137/17M1112236.
- [29] P. K. Jha, R. Lipton, Numerical convergence of finite difference approximations for state based peridynamic fracture models, *Computer Methods in Applied Mechanics and Engineering* 351 (2019) 184–225.
- [30] P. Jha, R. Lipton, Finite element approximation of nonlocal dynamic fracture models, *Discrete & Continuous Dynamical Systems-B* 26 (2021) 1675.
- [31] R. P. Lipton, P. K. Jha, Nonlocal elastodynamics and fracture, *Nonlinear Differential Equations and Applications NoDEA* 28 (2021) 1–44.
- [32] A. Coclite, G. M. Coclite, F. Maddalena, T. Politi, A numerical framework for nonlinear peridynamics on two-dimensional manifolds based

- on implicit $p\text{-(ec)}^k$ schemes, *SIAM Journal on Numerical Analysis* 62 (2024) 622–645. URL: <https://epubs.siam.org/doi/abs/10.1137/22M1498942>. doi:10.1137/22M1498942.
- [33] S. A. Silling, E. Askari, A meshfree method based on the peridynamic model of solid mechanics, *Computers & structures* 83 (2005) 1526–1535.
 - [34] X. Gu, Q. Zhang, X. Xia, Voronoi-based peridynamics and cracking analysis with adaptive refinement, *International Journal for Numerical Methods in Engineering* 112 (2017) 2087–2109.
 - [35] M. Bessa, J. Foster, T. Belytschko, W. K. Liu, A meshfree unification: reproducing kernel peridynamics, *Computational Mechanics* 53 (2014) 1251–1264.
 - [36] A. Javili, R. Morasata, E. Oterkus, S. Oterkus, Peridynamics review, *Mathematics and Mechanics of Solids* 24 (2019) 3714–3739.
 - [37] A. Shojaei, A. Hermann, C. J. Cyron, P. Seleson, S. A. Silling, A hybrid meshfree discretization to improve the numerical performance of peridynamic models, *Computer Methods in Applied Mechanics and Engineering* 391 (2022) 114544.
 - [38] S. Jafarzadeh, A. Larios, F. Bobaru, Efficient solutions for nonlocal diffusion problems via boundary-adapted spectral methods, *Journal of Peridynamics and Nonlocal Modeling* 2 (2020) 85–110.
 - [39] L. Lopez, S. F. Pellegrino, A spectral method with volume penalization for a nonlinear peridynamic model, *International Journal for Numerical*

- Methods in Engineering 122 (2021) 707–725. doi:<https://doi.org/10.1002/nme.6555>.
- [40] L. Lopez, S. F. Pellegrino, A space-time discretization of a nonlinear peridynamic model on a 2D lamina, Computers and Mathematics with Applications 116 (2022) 161–175. doi:<https://doi.org/10.1016/j.camwa.2021.07.004>.
- [41] L. Lopez, S. F. Pellegrino, A fast-convolution based space-time Chebyshev spectral method for peridynamic models, Advances in Continuous and Discrete Models 70 (2022). URL: <https://doi.org/10.1186/s13662-022-03738-0>. doi:<https://doi.org/10.1186/s13662-022-03738-0>.
- [42] L. Lopez, S. F. Pellegrino, A non-periodic Chebyshev spectral method avoiding penalization techniques for a class of nonlinear peridynamic models, International Journal for Numerical Methods in Engineering 123 (2022) 4859–4876. doi:<https://doi.org/10.1002/nme.7058>.
- [43] L. Lopez, S. F. Pellegrino, Computation of Eigenvalues for Nonlocal Models by Spectral Methods, Journal of Peridynamics and Nonlocal Modeling 5 (2023) 133–154. URL: <https://doi.org/10.1007/s42102-021-00069-8>. doi:10.1007/s42102-021-00069-8.
- [44] X. Liang, L. Wang, J. Xu, J. Wang, The boundary element method of peridynamics, International Journal for Numerical Methods in Engineering 122 (2021) 5558–5593.

- [45] N. Dimola, A. Coclite, G. Fanizza, T. Politi, Bond-based peridynamics, a survey prospecting nonlocal theories of fluid-dynamics, *Adv. Contin. Discrete Models* 2022 (2022) 26. doi:10.1186/s13662-022-03732-6, id/No 60.
- [46] G. M. Coclite, S. Dipierro, F. Maddalena, E. Valdinoci, Wellposedness of a nonlinear peridynamic model, *Nonlinearity* 32 (2018) 1–21. URL: <http://dx.doi.org/10.1088/1361-6544/aae71b>. doi:10.1088/1361-6544/aae71b.
- [47] B. Fornberg, G. Whitham, A numerical and theoretical study of certain nonlinear wave phenomena, *Philosophical Transactions of the Royal Society of London. Series A, Mathematical and Physical Sciences* 289 (1978) 373–404. URL: <https://royalsocietypublishing.org/doi/abs/10.1098/rsta.1978.0064>. doi:10.1098/rsta.1978.0064. arXiv:<https://royalsocietypublishing.org/doi/pdf/10.1098/rsta.1978.0064>.
- [48] C. Canuto, Boundary Conditions in Chebyshev and Legendre Methods, *SIAM Journal on Numerical Analysis* 23 (1986) 815–831. doi:<https://doi.org/10.1137/0723052>.
- [49] L. N. Trefethen, *Spectral Methods in MATLAB*, Society for Industrial and Applied Mathematics, 2000. URL: <https://epubs.siam.org/doi/abs/10.1137/1.9780898719598>. doi:10.1137/1.9780898719598. arXiv:<https://epubs.siam.org/doi/pdf/10.1137/1.9780898719598>.
- [50] C. Canuto, A. Quarteroni, Approximation results for orthogonal poly-

nomials in Sobolev spaces, *Math. Comp.* 38 (1982) 67–86. doi:<https://doi.org/10.1090/S0025-5718-1982-0637287-3>.

- [51] E. Hairer, C. Lubich, G. Wanner, Geometric numerical integration illustrated by the Störmer-Verlet method, *Acta Numerica* 12 (2003) 399 – 450. doi:<https://doi.org/10.1017/S0962492902000144>.